JOURNAL OF VIROLOGY, Nov. 1992, p. 6419–6428
0022-538X/92/116419-10$02.00/0

Vol. 66, No. 11

Subgenomic RNAs Mediate Expression of Cistrons Located Internally on the Genomic RNA of Tobacco Necrosis Virus Strain A

FRANK MEULEWAETER,[1]* MARC CORNELISSEN,[2] AND JOHN VAN EMMELO[2]†

Laboratorium voor Genetica, Universiteit Gent, K.L. Ledeganckstraat 35,[1] *and Plant Genetic Systems N.V.,*[2] *9000 Ghent, Belgium*

Received 20 April 1992/Accepted 4 August 1992

Upon infection of tobacco protoplasts, the genomic RNA of tobacco necrosis virus strain A (TNV-A) accumulates linearly in time. The accumulation patterns of the two subgenomic RNAs resemble those of endogenous mRNAs in that the peak levels are reached after several hours. The accumulation of the 1.3-kb subgenomic RNA is delayed by 1 h compared with that of the 1.6-kb subgenomic RNA, which illustrates the important role of the subgenomic RNAs in the regulation of TNV-A gene expression. The locations of the 5′ nucleotides of the subgenomic RNAs reveal that the 5′-proximal cistrons of the 1.6- and 1.3-kb RNAs encode an 8-kDa protein from open reading frame (ORF) 3 and the coat protein from ORF 5, respectively. In a wheat germ translation system, a synthetic transcript resembling the 1.6-kb RNA expresses both ORFs 3 and 4. Moreover, the synthesis of the 6-kDa protein from ORF 4 depends on the translation efficiency of ORF 3, suggesting that in vivo, ORFs 3 and 4 are both expressed from the 1.6-kb RNA. The major in vitro translation product of TNV-A genomic RNA is the coat protein. We show that the region upstream of the coat protein promotes internal initiation of translation in vitro. However, this region is functionally inactive in vivo, suggesting that TNV-A genomic RNA is not important for coat protein synthesis in plants.

Positive-strand RNA viruses produce during their infection cycle various species of viral RNA with specific functions. The genomic RNAs function as mRNAs for the expression of the 5′-proximal genes, which are often involved in viral replication. Furthermore, the genomic RNAs serve as templates for the synthesis of the viral negative strands, which direct the synthesis of genomic RNAs. At later stages of infection, the major part of these newly formed genomic RNAs is encapsidated by coat protein to form virus particles. Several viruses produce subgenomic RNAs to express cistrons which are positioned internally in the genome. It has been shown for some viruses that subgenomic RNAs arise by internal initiation of transcription on the minus strand in vitro (36, 42, 48) as well as in vivo (15, 39). The origin of minus strands corresponding to the subgenomic RNAs is less clear. They could arise either by degradation of the replicative intermediates during RNA isolation, by minus-strand synthesis on the subgenomic RNAs, or by premature termination of minus-strand synthesis on genomic RNA. There is no evidence that they serve as templates for the synthesis of subgenomic RNAs.

Tobacco necrosis virus (TNV) is a small icosahedral plant virus, belonging to the necrovirus group, with a single genomic RNA of about 4 kb. The RNA of TNV strain A (TNV-A) contains six major open reading frames (ORFs) (34) and most likely serves as mRNA for the synthesis of a 23-kDa protein and of a 82-kDa read-through protein, which are encoded by ORFs 1 and 2. In plants, the internal cistrons are most probably expressed from two 3′-coterminal subgenomic RNAs of 1.6 and 1.3 kb. These size estimates, together with hybridization analyses, suggest that the 5′ ends of the largest and smallest subgenomic RNAs are located upstream of ORFs 3 and 5, respectively (34). Subgenomic RNAs with ORF 4 or 6 as the 5′-proximal cistron have never been detected. A very similar genome organization was proposed for TNV-D (7) and for the carmovirus melon necrotic spot virus (40). The largest subgenomic RNA of TNV-A may serve as mRNA for an 8-kDa protein, whereas the smallest subgenomic RNA probably directs the synthesis of the viral coat protein. Interestingly, the major in vitro translation product of TNV-A genomic RNA is the coat protein, despite its location at the 3′ end of the RNA (34). However, the extent to which the genomic RNA contributes to coat protein expression in vivo is unresolved.

In this report, we address the question of how the internal cistrons of TNV-A are expressed in vivo. We show that the two subgenomic RNAs accumulate differently upon infection, suggesting a coordinated expression of the different cistrons. Furthermore, mapping of the 5′ nucleotides of the subgenomic RNAs confirmed that ORFs 3 and 5 are the 5′-proximal cistrons of the 1.6- and 1.3-kb RNAs, respectively. Translation of ORF 4 in vitro appeared to depend on the translation efficiency of ORF 3, which indicates that ORF 4 might be expressed in vivo from the 1.6-kb RNA. We also show that in vitro, TNV-A coat protein is synthesized from the genomic RNA by internal initiation of translation. However, the region supporting internal initiation of translation in vitro is functionally inactive in vivo. This finding suggests that TNV-A genomic RNA is not important for coat protein synthesis in plants.

MATERIALS AND METHODS

Plasmids. pFM17, pFM20, pFM21, pFM22, and pFM23 are in vitro transcription plasmids containing TNV-A cDNA clones (34). pFM119 is a nearly full-length TNV-A cDNA clone, made by recombining pFM22 and pFM20 at the unique *Nsi*I site (see Fig. 2C). pGEMBAR is an in vitro

* Corresponding author.
† Present address: Department of Bacteriology and Virology, University Hospital Gent, 9000 Ghent, Belgium.

transcription plasmid containing the bialorphos resistance (*bar*) gene (6). The transient expression plasmids pDE118 and pDE201 were kindly supplied by J. Denecke (Swedish University, Uppsala, Sweden). pGEM-3Z and pGEM-3Zf(+) were purchased from Promega Biotec (Madison, Wis.).

pFM150A contains TNV-A ORFs 3 and 4, as a 410-bp *Bcl*I-*Bam*HI fragment from pFM21, in the *Bam*HI site of pGEM-3Zf(+). The insert is oriented such that T7 RNA polymerase directs the synthesis of an RNA corresponding to the viral plus strand. TNV-A ORF 4 was inserted, as a 243-bp *Mbo*II-*Sph*I fragment from pFM21, between the *Sph*I and blunt-ended *Hin*dIII sites of pGEM-3Z, resulting in pFM126.

Plasmids pFM133 and pFM134 result from the insertion of the *bar* gene, as a 578-bp filled-in *Bam*HI fragment from pGEMBAR, into the blunt-ended *Sac*I site of pFM23 and pFM20, respectively. pFM143 was obtained by the insertion of a 625-bp *Sma*I-*Bsm*I fragment from pFM17 between the *Bsm*I and blunt-ended *Mlu*I sites of pFM134. This resulted in the deletion of 540 nucleotides (nt) of the TNV-A sequence compared with the pFM134 sequence.

The chloramphenicol acetyltransferase (*cat*) gene was placed, as a 775-bp *Xba*I–blunt-ended *Cla*I fragment from pDE118, between the *Xba*I and blunt-ended *Kpn*I sites of pGEM-3Z, resulting in plasmid pFM136. Insertion of the 1,427-bp blunt-ended *Eco*RI-*Pvu*I fragment from pFM134 into the blunt-ended *Sac*I site of pFM136 yielded plasmid pFM140. pFM139 was obtained by insertion of the *cat* gene, as a 792-bp *Pst*I–blunt-ended *Sac*I fragment from pFM136, between the *Pst*I and filled-in *Mlu*I sites of pFM134. A translational fusion between the coat protein gene and the *cat* gene was made by transfer of a 835-bp filled-in *Bam*HI fragment from pFM21 into the blunt-ended *Sac*I site of pFM136. The 1,371-bp *Pst*I-*Nsi*I fragment from the resulting plasmid was inserted between the *Pst*I and *Nsi*I sites of pFM134, giving rise to pFM138.

The transient expression plasmid pDE201 contains the *cat* coding region between the TR2′ promoter (46) and the 3′ end of the octopine synthetase gene (9) and the β-glucuronidase (*gus*) coding region between the TR1′ promoter and the T_L-DNA gene 7 fragment active in 3′ end formation and polyadenylation (45). pFM320 was produced by fill-in and self-ligation of the nonmethylated *Cla*I site of pDE201. In this way, the nucleotide context around the AUG codon of the *cat* mRNA is identical to the context found in the *cat* mRNA specified by pFM136 (cgcgaugg). The *cat* gene from pDE201 was replaced by the *bar* cistron by inserting a 562-bp blunt-ended *Nco*I-*Mlu*I fragment from pFM138 between the blunt-ended *Bst*XI and *Xba*I sites, yielding pFM321. Transient expression plasmids specifying dicistronic mRNAs were obtained by inserting the *Sal*I-*Eco*RI fragments from pFM139 and pFM140, respectively, between the *Sal*I site from pFM321 and the *Eco*RI site from pFM320, resulting in plasmids pFM322 and pFM324, respectively. Deletion of the blunt-ended *Bam*HI-*Dra*III fragment from pFM324 resulted in pFM331.

Protoplast inoculation. TNV-A genomic RNA was extracted with phenol from virus particles, which were purified from TNV-A-infected primary leaves of *Phaseolus vulgaris* (29). Tobacco protoplast preparation and inoculation were done essentially by the method of Gallie et al. (14), with an inoculum of 0.1 μg of TNV-A RNA for 10^6 protoplasts. After inoculation, the protoplasts were diluted 10-fold in the electroporation buffer of Fromm et al. (12), precipitated, and resuspended in the incubation medium (10) at a final concentration of 0.5×10^6 protoplasts per ml. Aliquots of 5×10^6 protoplasts were further incubated at 22°C in the dark.

RNA isolation, Northern (RNA) blotting and transcript mapping. RNA from protoplasts was prepared as described previously (10). The RNA was denaturated with glyoxal (33) and run on a formaldehyde–1.5% agarose gel as recommended by Amersham (Amersham, Buckinghamshire, England). Blotting, hybridization, and probe synthesis were also done according to Amersham's guidelines except that hybridization was at 68°C. Transcript levels were quantified by excision of the RNA band from the membrane and liquid scintillation counting of the probe which was bound to the transcript. The results were compared with those for a dilution series of a synthetic transcript.

RNA from bean leaves was isolated according to Jones et al. (21). Oligodeoxynucleotide primers were synthesized by a Gene Assembler Plus (Pharmacia LKB, Uppsala, Sweden). Primer extension assays were done essentially as described by McKnight et al. (32), with annealing at 50°C for 90 min. The primer extension products were analyzed in parallel with dideoxy termination sequencing ladders (41), generated with the same primers on plasmid pFM20. For the S1 nuclease protection assays, an SP6 transcript was synthesized by using *Nco*I-digested plasmid pFM17; 20 μg of this transcript was used as a template for cDNA synthesis, starting from a 5′-^{32}P-labeled oligodeoxynucleotide primer. The resulting cDNA was purified on a 6% acrylamide–urea gel and electroeluted. This cDNA probe was used in an S1 protection assay (3) after annealing during 5 h at 50°C with 1.5 μg of total RNA from infected and noninfected leaves. The same cDNA was used for the generation of a chemical sequencing ladder (31).

Transient expression and enzymatic assays. Tobacco protoplast isolation and plasmid DNA introduction were performed as previously described (10). RNA was isolated from 3.5×10^6 protoplasts 5 h after DNA delivery. At this time point, the RNA level has reached its steady-state level (not shown). Protein extracts were prepared from 1.5×10^6 protoplasts after 22 h of incubation (10). GUS assays were performed as described by Jefferson (20). Phosphinotricine acetyltransferase (PAT) activities were determined with 10 μg of soluble protein, using the thin-layer chromatography method of De Block et al. (8). Thin-layer chromatography CAT assays (16) were performed with 50 μg of soluble protein. TNV coat protein was detected by immunoblotting as described previously (35). The coat protein bands were quantified by measuring the color development with a Macroviewer (Joyce Loebl, Gateshead, England) and comparison with results for a dilution series of purified coat protein.

In vitro transcription and translation. In vitro RNA synthesis was done essentially by the method of Krieg and Melton (26). The reaction mixture contained 0.5 mM each nucleotide and 5 μM [^{14}C]ATP (500 nCi/mmol; Amersham). After incubation for 90 min at 37°C, additional nucleotides (0.3 mM) and T7 RNA polymerase were added, and synthesis was continued for 60 min. To synthesize capped transcripts, 0.5 mM cap analog [^{7}mG(5′)ppp(5′)G; Pharmacia] was included in the transcription mix, while the GTP concentration was lowered to 0.05 mM during the first 90 min of incubation. After synthesis was completed, the DNA template was removed with 0.3 U of DNase (RNase free; Boehringer, Mannheim, Germany) per μl. After phenolization, unincorporated nucleotides and cap analog were removed by passage through a Sephadex G-50 column. The RNA was precipitated with 0.2 M potassium acetate and 2 volumes of ethanol, and the resulting pellet was resuspended

in RNase-free water. The RNA concentration was measured by trichloroacetic acid precipitation on GF/C filters (Whatman, Maidstone, England) and liquid scintillation counting of the incorporated [^{14}C]AMP.

Wheat germ extract preparation and in vitro protein synthesis were carried out according to Morch et al. (37). Protein synthesis was done with final concentrations of 1 mM Mg^{2+} and 110 mM K^+. In vitro translation products were labeled with [^{35}S]methionine except when otherwise stated and separated on 12.5% polyacrylamide gels (27). Following electrophoresis, gels were fixed in 10% trichloroacetic acid, treated with En^{3}Hance (New England Nuclear, Boston, Mass.), and dried before autoradiography. The amount of protein synthesized was quantified by excision of the protein band from the dried gel and liquid scintillation counting. The values obtained were corrected for the number of methionine residues present in the protein species, excluding the initiator methionine.

RESULTS

TNV-A-specific RNAs have distinct accumulation profiles. Upon entry of TNV-A virions into susceptible plant cells, the genomic RNA is released and enters a viral replication program. Little is known about the initial phases of TNV-A infection. The expression strategy of the virus might to some extent be reflected by the timing of the production of the viral RNAs. We therefore determined the accumulation profiles of the various RNA species after TNV-A inoculation. A synchronized virus infection was achieved by electroporating tobacco protoplasts in the presence of purified TNV-A RNA. The accumulation of viral RNAs was monitored by Northern blot analysis of the 2 M LiCl-insoluble RNA from different time points, using RNA probes complementary to either the plus or minus strand of the subgenomic RNAs. Directly after RNA delivery, the protoplasts were washed to remove the extracellular RNA. As early as 30 min after viral RNA inoculation, we could not detect any intracellular viral RNA (Fig. 1A, lane 0).

The plus and minus strands of the genomic and largest subgenomic RNAs became detectable (>1 amol of RNA per μg of total RNA) after 3 h of incubation, whereas the smallest subgenomic RNA could be detected only after 4 h (Fig. 1A and B). As these amounts were too small for accurate quantitation, these time points are not included in Fig. 1C to E. The genomic TNV-A RNA accumulated linearly during the course of the experiment (Fig. 1C), indicating that the synthetic capacity of the protoplasts was not yet exhausted 33 h after infection. At that time point, 1 μg of total RNA contained 120 ng of viral RNA, 112 ng of which was genomic RNA. The accumulation rate of the genomic RNA was 323 transcripts per min per electroporated cell (r = 0.993). The accumulation rate per infected protoplast will be higher, as about 50% of the protoplasts die during the electroporation procedure and probably not all protoplasts will be infected. The almost linear increase in time of the genomic RNA during the first 33 h after inoculation can be explained by the stabilization of the major part of the synthesized genomic RNA through encapsidation by coat protein. Therefore, we determined the amount of coat protein in the infected protoplasts by immunoblotting. The coat protein became detectable (>15 ng/15 μg of soluble protein) after 8 h of incubation, whereafter it accumulated almost linearly in time (Fig. 1F). At all time points, the amount of coat protein was 1.4 to 2.0 times the amount necessary for the encapsidation of all genomic TNV-A RNA, suggesting that the major part of this RNA is encapsidated. There is obviously a complex equilibrium between the pool sizes of free genomic RNA, minus-strand RNA, and subgenomic RNAs and the production of coat protein, which removes the free genomic RNA and thus indirectly controls the level of the other RNA species.

The accumulation profiles of the subgenomic RNAs appear similar to those of endogenous mRNAs (2). After about 25 h of incubation, the subgenomic RNAs reached their peak levels (Fig. 1D), suggesting a turnover rate in the range of hours (2). Interestingly, the accumulation of the smallest subgenomic RNA was delayed by 1 h compared with that of the largest one. As the subgenomic RNAs are not encapsidated into virus particles, this finding also means that the largest subgenomic RNA becomes available for translation at an earlier stage of infection, which probably leads to a significant synthesis of its translation product(s) before the appearance of the coat protein. In an early stage of infection, the accumulation rate of the genomic RNA exceeded the synthesis rate of the subgenomic RNAs by two- to threefold. A similar situation was found for the accumulation of the three minus-strand RNAs (Fig. 1E). Again, the full-length minus-strand RNA accumulated about two- to threefold faster than did the subgenomic RNAs, but in contrast with the genomic RNA, its level stabilized after 6 h of incubation at about 1,500 molecules per cell. As the accumulation rate of the genomic RNA was about 300 molecules per min, this finding implies that at least 0.2 genomic RNA is synthesized per minus-strand RNA per min. The full-length minus-strand RNA reached its steady-state level shortly after the appearance of the smallest subgenomic RNA, which is probably the mRNA that encodes the coat protein. This result is in agreement with the idea that the encapsidation of the genomic RNA controls minus-strand synthesis by reducing the amount of free genomic RNA. The minus strands of the subgenomic RNAs accumulated to levels similar to that of the full-length minus strand, although they reached the peak level at a later time point, suggesting that these RNAs are less efficiently produced but more stable or are synthesized from another, more accessible substrate, e.g., the corresponding subgenomic RNAs. Figure 1E also shows that the 1.3-kb minus-strand RNA accumulated with a time delay relative to the 1.6-kb minus-strand RNA, which is similar to that of the corresponding plus strands. This finding indicates that the accumulations of the plus and minus strands of the subgenomic RNAs are somehow interdependent.

The 5′ sites of the subgenomic RNAs map at conserved regions. Size estimations and hybridization analyses indicated that the 5′ ends of the subgenomic RNAs of TNV-A are located upstream of ORFs 3 and 5 (34). As the exact location of these sites reveals part of the translation strategy of the virus, we mapped the 5′ ends of the subgenomic RNAs of TNV-A more precisely. Primer extension assays were performed with total RNA from TNV-A-infected bean leaves, and the extension products were compared with transcripts obtained with total RNA from healthy control plants to which TNV-A RNA from purified virions was added. This latter control was included to discriminate between artificial termination sites and sites specific for the 5′ ends of the subgenomic RNAs.

Primer extension with a primer complementary to nt 2442 to 2461 of TNV-A RNA yielded several transcripts in both reactions. Only one extension transcript was more abundant in the reaction with RNA from infected plants than in the reaction with the control. The specific transcript stopped at nt 2184 of TNV-A genomic RNA (Fig. 2A). We also mapped

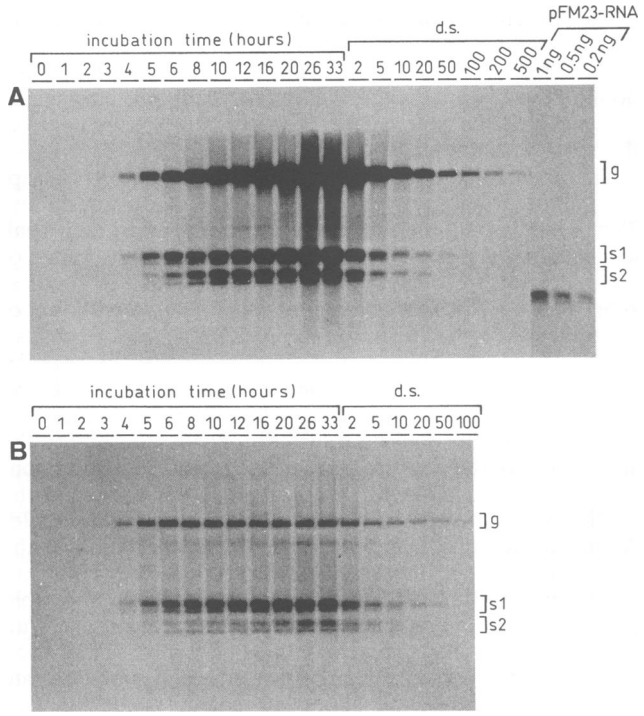

FIG. 1. Accumulation of TNV-A-specific RNAs and coat protein in infected tobacco protoplasts. Time point samples are indicated by the time of incubation (in hours), starting 30 min after electroporation. The extraction of 10^6 electroporated protoplasts yielded approximately 10 μg of single-stranded RNA or 150 μg of soluble protein. (A) Northern blot probed with an RNA complementary to nt 2057 to 3660 of TNV-A RNA, showing the accumulation of the TNV-A plus-strand RNAs (2-h exposure). Each lane was loaded with 1 μg of single-stranded RNA. d.s., dilution series of the RNA from the last time point sample. Numbers indicate the dilution factors. pFM23-RNA was synthesized from *Hin*dIII-digested pFM23 DNA, using T7 RNA polymerase. The synthetic transcript and the RNA from the dilution series were adjusted to 1 μg with single-stranded RNA from healthy tobacco leaves. g, genomic RNA; s1 and s2, 1.6- and 1.3-kb subgenomic RNAs. The subgenomic RNAs and the synthetic transcript do not migrate as a single band. We attribute this to an artifact occurring during electrophoresis or blotting, since the same RNA samples on other gels did not show this artifact. (B) Northern blot probed with an RNA corresponding to nt 2593 to 3510 of TNV-A RNA, showing the accumulation of the TNV-A minus-strand RNAs (15-h exposure). (C) Accumulation of TNV-A plus-strand RNAs. ○, genomic RNA; □, 1.6-kb subgenomic RNA; ◇, 1.3-kb subgenomic RNA. (D) Accumulation of TNV-A subgenomic RNAs compared with the accumulation of the genomic RNA early during infection. (E) Accumulation of TNV-A minus-strand RNAs. (F) Accumulation of TNV-A coat protein between 8 and 16 h after inoculation.

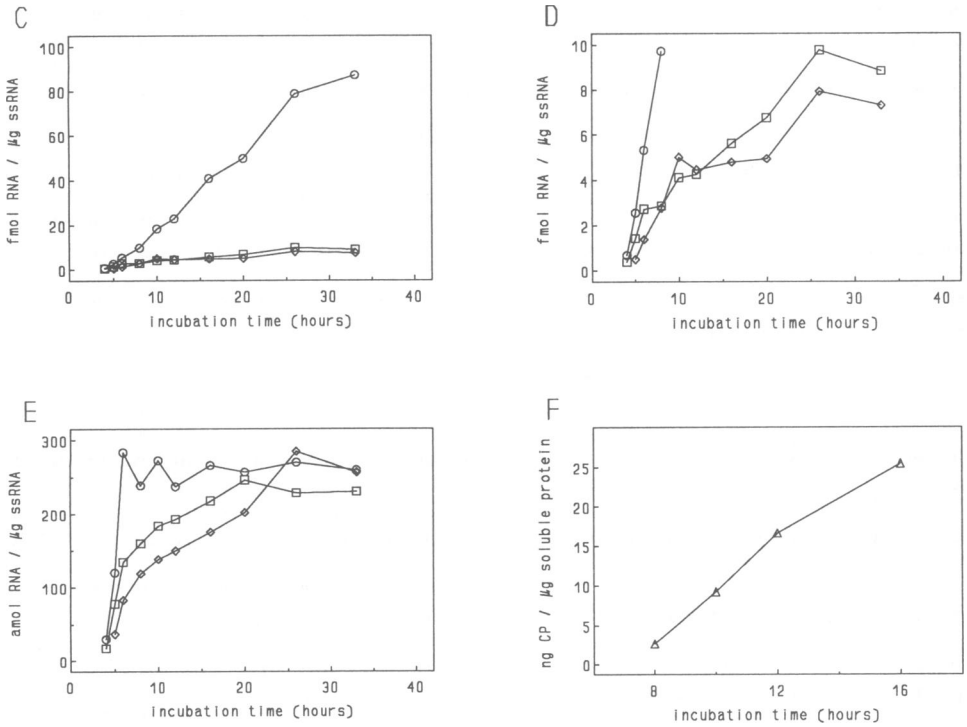

this 5′ site by S1 analysis, which resulted in the protection of nt 2184 as well as nt 2183 to 2180 (not shown). This latter protection probably results from the intramolecular base-pairing ability of the 6 nt directly upstream of nt 2184. The transcript corresponding with nt 2184 of TNV-A RNA agrees well with a termination product for the 1.6-kb RNA, as it implicates a leader sequence of 48 nt upstream of the start codon of ORF 3 (Fig. 2C).

Primer extension reactions with a primer complementary to nt 2657 to 2679 of TNV-A RNA yielded one subgenomic RNA specific transcript of about 220 nt (Fig. 2B). However, this transcript migrated on a sequencing gel between the dideoxy termination products corresponding to nt 2460 and 2461 of TNV-A RNA. To determine the 5′ nucleotide of the 1.3-kb RNA more precisely, an S1 nuclease protection assay was performed with a cDNA probe complementary to nt

2302 to 2679 of TNV-A RNA. The same cDNA was used to generate a sequencing ladder by the chemical method (31). In this way, migration differences between the sequencing ladder and the subgenomic RNA-specific DNA fragment were excluded. The S1 mapping yielded one major fragment, which was protected up to nt 2461 of TNV-A RNA (Fig. 2B). This result is in good agreement with the previous estimates for the smallest subgenomic RNA. The 1.3-kb RNA has a leader of 152 nt, with a G content of only 11.8%, that precedes the start codon of the coat protein gene (Fig. 2C).

To identify conserved primary sequences that could be involved in the synthesis of subgenomic RNAs, the sequences surrounding the start sites of both subgenomic RNAs were aligned (Fig. 2D). Substantial sequence similarity (15 of 20 nt) was found between nt −1 and +19 relative to the initiation sites, which are designated +1. In contrast, for the related carnation mottle virus (CarMV), the sequence similarity between the two subgenomic promoters is located almost exclusively upstream of the initiation sites (4). Interestingly, there is significant sequence similarity between the sequences surrounding the initiation sites of the 1.6-kb RNA of TNV-A and the 1.5-kb RNA of CarMV (13 of 18 nt between −11 and +7).

Identification of in vitro translation products of ORFs 3 and 4. Mapping of the 5′ sites of the subgenomic RNAs showed that ORF3 is the most 5′-proximal ORF of the 1.6-kb subgenomic RNA, whereas ORF 4 is the second cistron. TNV-D and the carmoviruses have ORFs similar to ORFs 3 and 4 of TNV-A at the same genome location (7, 40). For the carmovirus turnip crinkle virus, both ORF 3 and 4 are required for cell-to-cell transport. Moreover, the putative proteins encoded by both TNV-A ORFs share some limited sequence similarity with the putative proteins from the corresponding ORFs of the other viruses, which supports their functional significance. However, it is not clear whether and how TNV-A expresses ORF 4 during infection, as a subgenomic RNA with ORF 4 as the 5′-proximal cistron could not be detected. To gain further insight into the possible translation strategy of ORF 4, the in vitro translation products of synthetic transcripts covering different parts of the central genomic region of TNV-A were analyzed (Fig. 3).

The translation products of ORFs 3 and 4 can be easily distinguished by labeling with different radioactive amino acids, since the 8-kDa protein of ORF 3 lacks proline residues whereas ORF 4 has, apart from the initiation codon, no methionine codons. Indeed, a synthetic transcript which contains only ORF 4 (pFM126) directs the synthesis of a small polypeptide that is detected only after labeling with [^{3}H]proline and not with [^{35}S]methionine (Fig. 3). This result indicates that the initiating methionine residue is posttranslationally removed in the wheat germ translation system. A synthetic transcript derived from pFM150A, which covers both ORFs 3 and 4, directs the synthesis of two methionine-containing polypeptides with apparent molecular masses of 15.3 and 16.6 kDa (Fig. 3). The faster-migrating protein is about 10 times more abundant than the larger one. Both proteins originate from ORF 3, since they incorporate

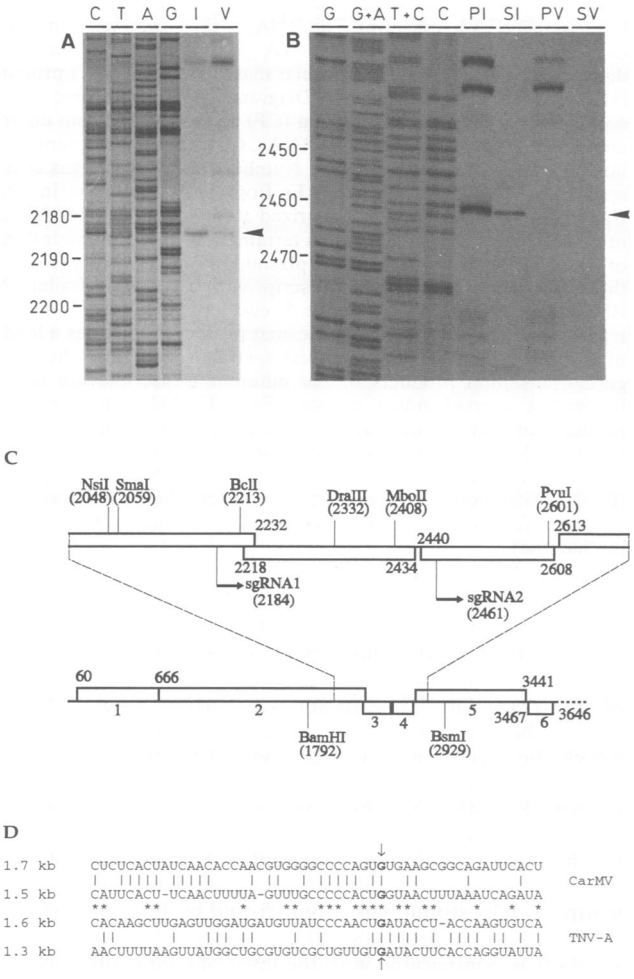

FIG. 2. Mapping of the 5′ nucleotides of TNV-A subgenomic RNAs. (A) Primer extension mapping of the 5′ nucleotide of the 1.6-kb subgenomic RNA. The extension reaction was performed with a primer complementary to nt 2442 to 2461 of TNV-A RNA and 5 μg of single-stranded RNA from TNV-A infected *Phaseolus* leaves (lane I) or from healthy control plants, supplemented with 0.1 μg of TNV-A RNA from purified virus particles (lane V). The subgenomic RNA-specific extension product is indicated with an arrow. Lanes G, A, T, and C contain the products of a dideoxy termination sequencing reaction performed with the same primer on plasmid pFM20. Numbers at the left indicate the positions of the corresponding nucleotides on TNV-A genomic RNA. (B) Mapping of the 5′ nucleotide of the 1.3-kb subgenomic RNA. Primer extension reactions were performed with a primer complementary to nt 2657 to 2679 of TNV-A RNA and with the same RNAs as in panel A (lanes PI and PV). The same RNAs were also used for S1 nuclease mapping with a cDNA complementary to nt 2302 to 2679 of TNV-A RNA (lanes SI and SV). The other lanes contain a Maxam-and-Gilbert sequencing ladder of the cDNA used for the S1 mapping. (C) Genome map of TNV-A with the locations of the 5′ sites of the subgenomic RNAs and of the relevant restriction sites. All restriction sites are unique for the TNV-A sequence except *Mbo*II, *Bam*HI, and *Bsm*I, for which only the location relevant for the cloning strategies is indicated. Numbers in parentheses indicate the corresponding nucleotides of the TNV-A sequence (34). Boxes represent the ORFs, which are drawn to scale. The numbers of the ORFs as used in the text are indicated below the boxes. The first nucleotide of the relevant start and stop codons is also indicated. The dashed line represents the 3′ end of the genomic RNA, which was not sequenced. (D) Sequence conservation near the 5′ nucleotides of the subgenomic RNAs of CarMV and TNV-A. Bars indicate nucleotides conserved between the two subgenomic RNAs of the same virus. Asterisks indicate nucleotides conserved between the 1.5-kb RNA of CarMV and the 1.6-kb RNA of TNV-A. Arrows indicate the 5′ nucleotides of the subgenomic RNAs.

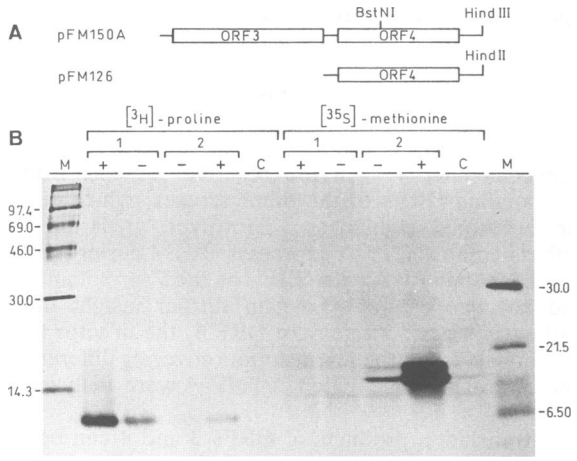

FIG. 3. Characterization of in vitro translation products of TNV-A ORFs 3 and 4. (A) Diagram of the synthetic RNAs used to characterize the in vitro translation products of ORFs 3 and 4. The names of the in vitro transcription plasmids are indicated at the left. (B) Wheat germ translation products of the RNAs shown in panel A. Each lane contains the translation products of 0.75 pmol of RNA, with (+) or without (−) 5′ cap, in a 12.5-μl wheat germ reaction. Proteins were labeled with [^{3}H]proline or [^{35}S]methionine. 1, RNA from *Hin*dII-digested pFM126; 2, RNA from *Hin*dIII-digested pFM150A; C, control with no added RNA. Molecular masses of the marker proteins (M) are indicated in kilodaltons.

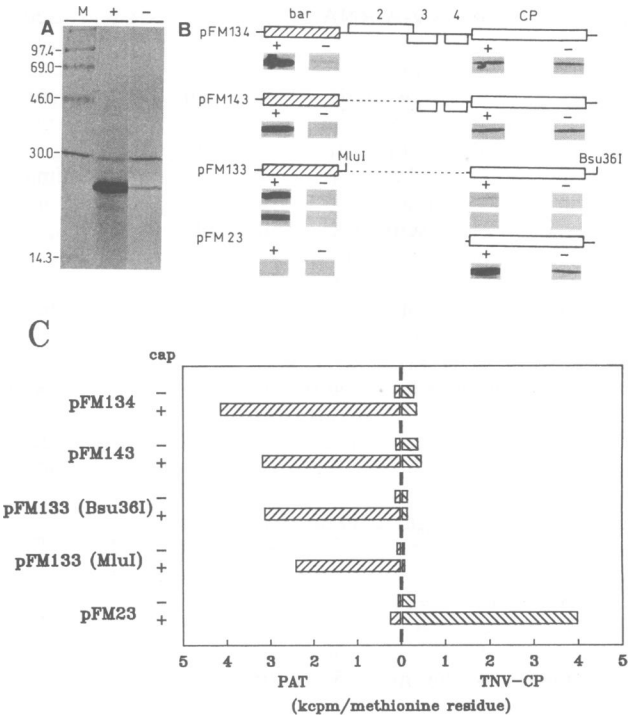

FIG. 4. Internal initiation of translation of TNV-A coat protein in vitro. (A) Wheat germ translation products of a synthetic almost full-length TNV-A transcript. The RNA, with (+) and without (−) 5′ cap, was synthesized with T7 RNA polymerase from the *Sal*I-digested plasmid pFM119. Molecular masses of the marker proteins (M) are given in kilodaltons. (B) Diagrams of the dicistronic RNAs containing the coat protein cistron (CP) as the downstream cistron and of the monocistronic control RNAs. Cistrons are represented by boxes, which are drawn to scale. Numbers above the boxes correspond to the numbers of the ORFs from TNV-A. Before in vitro transcription, plasmids were linearized at the unique *Bsu*36I site, 30 nt downstream of the coat protein termination codon. For synthesis of the monocistronic *bar* mRNA, plasmid pFM133 was linearized at the *Mlu*I site, resulting in a transcript with a 9-nt-long trailer. All RNAs with the *bar* cistron at the 5′ end have the same 16-nt-long leader, whereas the monocistronic coat protein mRNA has a leader of 42 nt, including 19 nt of its natural upstream sequence. The wheat germ translation products of the different transcripts are shown below the corresponding cistron. For pFM133, the translation products of both the dicistronic RNA (first row) and the transcript terminated at the *Mlu*I site (second row) are shown. The fluorograph film was exposed for 16 h. +, capped RNA; −, RNA without 5′ cap. (C) Quantification of the translation products shown in panel B, in 10^3 cpm (kcpm) per methionine residue (excluding the initiator methionine).

[^{35}S]methionine and not [^{3}H]proline, and are also synthesized from a pFM150A transcript which ends 36 nt downstream of the stop codon of ORF 3 (not shown). Interestingly, Jones and Reichmann (22) detected the induction of a 15-kDa protein in tobacco leaves upon TNV infection. This protein might correspond to the translation product of ORF 3.

The full-length capped pFM150A transcripts also directed the synthesis of the proline-containing polypeptide from ORF 4. However, this protein was not detected upon translation of the uncapped pFM150A transcript (Fig. 3B). This result shows that in vitro, the translation of ORF 4 depends on the translation efficiency of ORF 3, which suggests that ORF 4 might be expressed in vivo from the 1.6-kb RNA. However, a protein corresponding to the ORF 4 gene product has not been detected in TNV-infected plants.

TNV-A genomic RNA directs coat protein synthesis in vitro by internal initiation of translation. The coat protein is the major in vitro translation product of TNV-A genomic RNA, despite the location of the coat protein cistron at the 3′ end of the RNA (34). Although there are no data available on the in vivo translation products of genomic TNV RNA, the coat protein is most likely synthesized from the 1.3-kb subgenomic RNA. To elucidate the role of the genomic RNA in TNV-A coat protein synthesis, we studied the mechanism of coat protein synthesis in vitro and investigated whether the same mechanism is active in vivo.

An in vitro-synthesized transcript that covers almost the complete genome of TNV-A directs, in a wheat germ translation system, the synthesis of the same proteins as does the genomic RNA with also predominantly the coat protein (34). This finding implies that in vitro, the coat protein is indeed synthesized from the genomic RNA and not from small RNAs contaminating the virus preparation. A cap structure at the 5′ end of the in vitro TNV-A transcripts stimulated in vitro the translation of the 23-kDa protein from the 5′ ORF about ninefold, whereas coat protein synthesis was slightly reduced (Fig. 4A). This result shows that coat protein synthesis in vitro does not depend on the efficient translation of the 5′ cistron. This matter was further investigated by testing the translational capacities of dicistronic RNAs in which the coat protein cistron, with different lengths of its upstream sequence, was placed downstream of the *bar* cistron (Fig. 4B). The *bar* gene encodes the PAT protein. Each of the dicistronic transcripts directed coat protein synthesis in a fashion independent of the presence of a cap structure at the 5′ end of the transcript, whereas PAT synthesis was stimulated about 25-fold by the cap (Fig. 4C). The level of coat protein synthesis directed by the dicistronic RNAs was comparable with the level of coat protein synthe-

sis of a monocistronic mRNA lacking a cap structure. Only the dicistronic RNA in which the coat protein cistron is preceded by 19 nt of its own upstream sequence showed a lower coat protein synthesis. This result shows that in vitro, a sequence of 309 nt upstream of the coat protein coding region increases the frequency of internal initiation of translation by threefold.

Discrete TNV-A fragments stimulate internal initiation of translation in vitro but not in vivo. To examine the autonomy of the upstream region to stimulate internal initiation of translation in vitro, we constructed plasmids for the in vitro synthesis of dicistronic RNAs in which the coat protein cistron was replaced by the *cat* coding region (Fig. 5A). The translation efficiencies of the different cistrons were again tested in a wheat germ translation system. PAT synthesis was about the same for all dicistronic RNAs and was strongly stimulated on transcripts having a cap structure at their 5′ ends; in contrast, translation of the downstream *cat* cistron was not enhanced by a cap structure at the 5′ end of the RNA (Fig. 5B). Moreover, detectable levels of CAT protein were synthesized only when the *cat* cistron was preceded by the TNV-A fragment. This internal initiation of translation was not caused by a specific cleavage of the dicistronic RNA, as no discrete degradation products arose during translation and the dicistronic RNAs had a similar chemical stability in the wheat germ translation system ($t_{1/2}$ = 32 to 38 min; not shown). The initiation context of the coat protein gene appeared not to be essential, as RNA derived from pFM140 directed the same level of CAT synthesis as did RNA from pFM138. The level of CAT synthesis by internal initiation was comparable to the level of synthesis from the uncapped monocistronic *cat* mRNA, which was about 35-fold less than the level of synthesis from a monocistronic *cat* mRNA having a cap structure at the 5′ end. These results clearly show that the 850-nt sequence upstream of the coat protein gene is capable of enhancing internal initiation of translation in vitro. Similar results were obtained with an *npt*II cistron instead of *cat* (not shown).

To test whether the 300-nt TNV-A sequence also stimulates internal initiation of translation in vivo, we constructed transient expression plasmids which specify, under the control of the TR2′ promoter, dicistronic RNAs comparable with those tested in vitro (Fig. 6). The different plasmids were introduced into tobacco mesophyl protoplasts by electroporation, and expression of both the *bar* and *cat* genes was monitored at the RNA and protein levels. Experimental variation was corrected for by the expression level of the *gus* gene, which was under the control of the TR1′ promoter. Table 1 shows the results of a representative transient expression experiment. The PAT activity specified by the 5′ cistron of the dicistronic constructs was at least 10 times lower than the PAT activity directed by the monocistronic control (pFM321). This finding can be partly explained by the lower steady-state levels of the dicistronic RNAs. The remaining differences might be caused by a lower level of reinitiation of translation, as the *cat* gene and the intercistronic region are placed between the *bar* termination codon and the poly(A) tail, which is involved in reinitiation of translation (38). The dicistronic RNAs specified without exception a very low level of CAT activity (400 to 500 pg of CAT per mg of soluble protein), and stimulation of CAT synthesis because of the intercistronic TNV-A sequence was not observed. This finding shows that the requirements for internal initiation of translation in vivo differ from the requirements in vitro. It is thus unlikely that TNV-A genomic RNA serves as mRNA for the synthesis of the coat

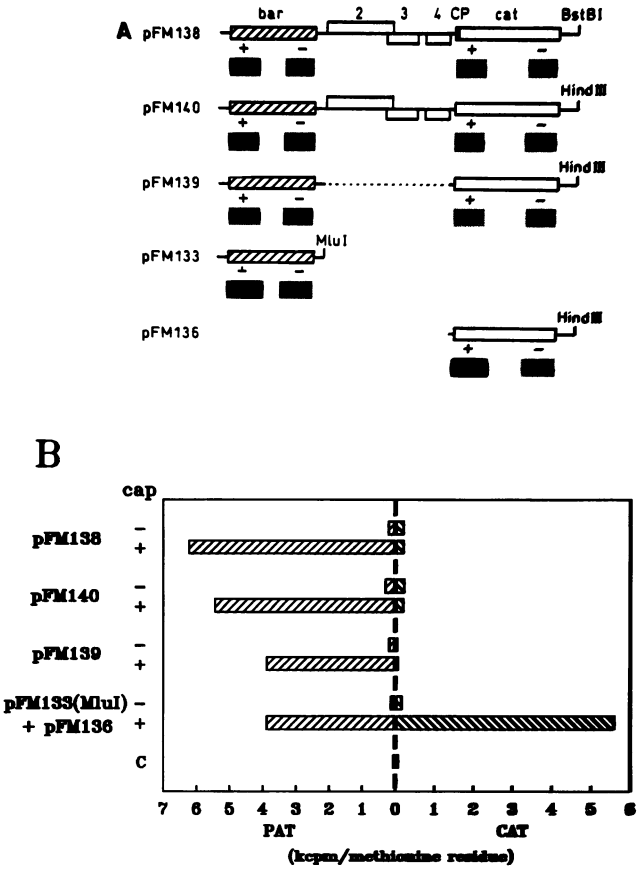

FIG. 5. Stimulation of internal initiation of translation in vitro by a discrete TNV-A fragment. (A) Diagrams of the mono- and dicistronic RNAs containing the *bar* and *cat* cistrons. Cistrons are represented by boxes, which are drawn to scale. Numbers above the boxes correspond to the numbers of the ORFs from TNV-A. The restriction enzymes which were used to digest the plasmids before in vitro transcription are indicated. All RNAs with the *bar* cistron at the 5′ end have the same 16-nt-long leader except for the pFM140 RNA, which contains a 6-nt insertion in the leader. The monocistronic *cat* mRNA has a leader of 19 nt. The wheat germ translation products of the different transcripts are shown below the corresponding cistron. The fluorograph film was exposed for 18 h. +, capped RNA; −, RNA without 5′ cap; CP, coat protein cistron. (B) Quantification of the translation products shown in panel A, in 10^3 cpm (kcpm) per methionine residue (excluding the initiator methionine). C, control with no added RNA.

protein in vivo unless *cis*-acting sequences in addition to those that are essential in vitro are required for internal initiation in vivo. The lack of internal initiation on the dicistronic RNAs in vivo is not due to the absence of *trans*-acting factors induced by virus infection, since a stimulation of CAT synthesis was not observed upon cointroduction of TNV-A RNA (not shown).

DISCUSSION

The expression strategy of TNV-A upon infection is largely unknown. We studied the regulatory features of the internal cistrons at both the transcriptional and translational levels. The regulation of accumulation of viral RNAs is a complex process. As TNV-A genomic RNA is stabilized by encapsidation into virus particles, it accumulated linearly

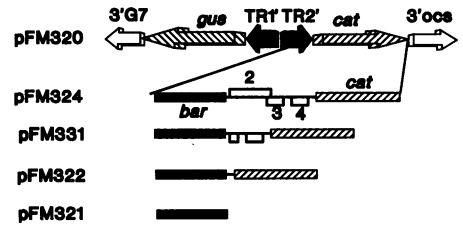

FIG. 6. Diagrams of the chimeric genes from the transient expression plasmids which were used to test the ability of a discrete TNV-A fragment to stimulate internal initiation of translation in vivo. TR1' and TR2' refer to the dual TR promoter (46); 3'G7 and 3' ocs indicate the fragments active in 3' end formation and polyadenylation from the T_L-DNA gene 7 (45) and the octopine synthase gene (9), respectively. Cistrons are represented by boxes, which are drawn to scale. Numbers above and below the boxes correspond to the numbers of the ORFs from TNV-A.

during the course of the experiment. In contrast, the subgenomic RNAs accumulated, like endogenous mRNAs, toward an equilibrium between synthesis and degradation. Up-regulation of plus-strand accumulation by the coat protein has been implicated for tobacco mosaic virus (TMV) (19), brome mosaic virus (30), and alfalfa mosaic virus (44). However, the accumulation profile of TMV genomic RNA differs essentially from that of TNV-A RNA, as its accumulation rate decreases after 8 h of infection. This difference might be caused by the fact that at least 70% of the TMV genomic RNA is not encapsidated and is consequently susceptible to degradation. In the case of TNV-A, however, the fraction of genomic RNA that is encapsidated was not determined, but the amount of coat protein in the protoplasts is in principle sufficient to encapsidate most of the genomic RNAs.

Accumulation of the full-length minus-strand TNV-A RNA ceased after 6 h of incubation, possibly because of the encapsidation of the genomic RNA, which stabilizes minus-strand synthesis. A similar stop of accumulation of minus-strand RNA was observed with TMV-infected protoplasts (19). A TMV deletion mutant lacking the 30-kDa protein and the coat protein genes reaches this equilibrium only 2 h later, which suggests that the minus-strand steady-state level is determined by other factors as well.

The main difference between the accumulation patterns of the two subgenomic TNV-A RNAs is a 1-h delay of the smallest subgenomic RNA compared with the largest one. A possible explanation is that the presence of the 1.6-kb RNA or of its translation products is required for synthesis of the 1.3-kb RNA. Otherwise, this difference could result from a difference in the activity of the subgenomic promoters early during infection. For brome mosaic virus and alfalfa mosaic virus, the regions involved in subgenomic promoter activity have been mapped to sequences both upstream and downstream of the start sites of the subgenomic RNAs (11, 43). In the case of TNV-A, sequence similarity is essentially found downstream of the start sites of the two subgenomic RNAs, whereas for CarMV, this similarity is mainly located upstream of the initiation sites. The sequence conservation around the start sites of the 1.5-kb RNA of CarMV and the 1.6-kb RNA of TNV-A and the similarity between their putative polymerases suggest that these viruses have similar mechanisms for subgenomic RNA synthesis. The fact that a certain sequence conservation is located upstream of the start sites also points toward a role for the upstream sequences in TNV-A subgenomic RNA synthesis. The lack of sequence similarity in this region between the two subgenomic RNAs of TNV-A could be important for the differences in accumulation between the two subgenomic RNAs, as observed early during infection.

TABLE 1. Transient expression of *bar* and *cat* genes from dicistronic RNAs in tobacco protoplasts

Plasmid	RNA concn (amol/μg of total RNA)	Relative PAT activity	PAT/RNA	Relative CAT activity	CAT/RNA
pFM320	310			100	100
pFM321	860	100	100	0.05	
pFM322	181	10	48	0.15	0.26
pFM331	322	7.7	21	0.13	0.13
pFM324	228	5.0	19	0.13	0.18

The difference in subgenomic RNA accumulation may have important implications for the TNV-A infection cycle, as the coat protein is probably synthesized only after the appearance of the translation products of the 1.6-kb subgenomic RNA. The location of the 5' end of this RNA indicates that it codes in vivo for the 8-kDa protein from ORF 3. Moreover, in vitro translation experiments show that the translation of ORF 4 depends on the translation efficiency of ORF 3. This finding suggests a role of the 1.6-kb RNA in synthesis of the 6-kDa protein from ORF 4 in vivo. Initiation of translation of ORF 4 by leaky scanning (24) is unlikely, as the initiation codon of ORF 4 is preceded by six other AUGs, several of which are in a context favorable for translation initiation (23). If ORF 4 is translated in vivo, the most likely mechanism is that translation reinitiates after translation of ORF 3. The only plant virus for which such a translation strategy has been demonstrated in vivo is cauliflower mosaic virus (13). Obviously, the mechanism of expression of TNV-A ORF 4 has to be investigated further in vivo.

The translation products of TNV-A ORFs 3 and 4 show limited sequence similarity with the proteins of the corresponding ORFs of TNV-D and the carmoviruses (7, 40). In the case of turnip crinkle virus, both proteins are required for viral cell-to-cell transport (17). The TNV-A 8- and 6-kDa proteins may, therefore, play a role in virus transport. In the case of TMV, the I_2 subgenomic RNA, which codes for the 30-kDa movement protein (P30), is detected only up to 10 h after inoculation, whereas the coat protein mRNA is synthesized continuously (47). Consequently, synthesis of the 30-kDa protein is not detected later than 12 h postinoculation. Moreover, insertion of coat protein RNA promoter sequences upstream of the TMV P30 coding sequence results in delay of expression and causes deficiency in cell-to-cell movement of the mutant virus (28). It was proposed that the TMV movement protein has to be expressed at an early stage of infection to efficiently compete with the coat protein for TMV RNA binding in order to form P30-TMV RNA transport complexes (5). The 1-h delay of the TNV-A coat protein mRNA compared with the mRNA for the putative TNV-A transport proteins would be compatible with a similar mechanism.

The smallest subgenomic RNA of TNV-A codes for the coat protein, which is the most abundant protein synthesized during TNV infection (22). In infected protoplasts, the rate of coat protein accumulation between 8 and 16 h after infection varies between 300 and 360 molecules per 1.3-kb RNA molecule per h. This means that at least one coat protein molecule per mRNA was synthesized every 10 to 12

s. This is in the range reported for efficiently translated mRNAs in mammals, which initiate protein synthesis once every 5 to 6 s (18). Interestingly, the subgenomic RNAs are probably, in analogy with the genomic RNA, not capped, as the primer extension products of the subgenomic RNAs consist of one single band and not of two bands as is often observed for capped RNAs (reference 49 and references therein). This finding implies that in vivo cap-independent translation initiation can be very efficient and that the 1.3-kb RNA must contain sequences that compensate for the absence of the cap structure. These same sequences might contribute to the efficient internal initiation of translation at the coat protein cistron on the genomic RNA in vitro. Moreover, the mechanism of coat protein synthesis in vitro differs essentially from the translation of ORF 4 from dicistronic RNAs, as coat protein synthesis proved to be completely independent of translation of the 5′ cistron. This internal initiation of translation requires at most 309 nt of the upstream sequence and is also observed when the coat protein cistron is replaced by a marker cistron (*cat*). However, the translation efficiency of the downstream cistron in transient expression is about 0.13 to 0.26% of the efficiency of the monocistronic mRNA, comparable with the translation efficiencies of downstream cistrons of dicistronic RNAs observed previously by Angenon et al. (1). Moreover, stimulation of translation of the downstream cistron by intercistronic TNV-A sequences was not observed in transient expression assays, which indicates that the internal initiation of translation directed by the region upstream of the coat protein cistron is typical for the in vitro translation system, despite the fact that the conditions for the wheat germ translation reaction were chosen to minimize artificial initiation of translation (25). Although internal initiation might require *cis*-acting sequences in vivo in addition to those essential in vitro, it is very likely that in vivo TNV-A genomic RNA does not act as a polycistronic mRNA and that TNV-A coat protein is synthesized mainly from the 1.3-kb subgenomic RNA.

ACKNOWLEDGMENTS

We thank Jef Seurinck, Karel Spruyt, and Vera Vermaercke for technical help and Jürgen Denecke for the gift of some plasmids.

Frank Meulewaeter is a research assistant of the National Fund for Scientific Research (Belgium).

REFERENCES

1. **Angenon, G., J. Uotila, S. A. Kurkela, T. H. Teeri, J. Botterman, M. Van Montagu, and A. Depicker.** 1989. Expression of dicistronic transcriptional units in transgenic tobacco. Mol. Cell. Biol. **9**:5676–5684.
2. **Brandhorst, B. P., and E. H. McConkey.** 1974. Stability of nuclear RNA in mammalian cells. J. Mol. Biol. **85**:451–463.
3. **Calzone, F. J., R. J. Britten, and E. H. Davidson.** 1987. Mapping of gene transcripts by nuclease protection assays and cDNA primer extension. Methods Enzymol. **152**:611–632.
4. **Carrington, J. C., and T. J. Morris.** 1986. High resolution mapping of carnation mottle virus-associated RNAs. Virology **150**:196–206.
5. **Citovsky, V., and P. Zambryski.** 1991. How do plant virus nucleic acids move through intercellular connections? BioEssays **13**:373–379.
6. **Cornelissen, M., and M. Vandewiele.** 1989. Both RNA level and translation efficiency are reduced by anti-sense RNA in transgenic tobacco. Nucleic Acids Res. **17**:833–843.
7. **Coutts, R. H. A., J. E. Rigden, A. R. Slabas, G. P. Lomonossoff, and P. J. Wise.** 1991. The complete nucleotide sequence of tobacco necrosis virus strain D. J. Gen. Virol. **72**:1521–1529.
8. **De Block, M., J. Botterman, M. Vandewiele, J. Dockx, C. Thoen, V. Gosselé, N. Rao Movva, C. Thompson, M. Van Montagu, and J. Leemans.** 1987. Engineering herbicide resistance in plants by expression of a detoxifying enzyme. EMBO J. **6**:2513–2518.
9. **De Greve, H., P. Dhaese, J. Seurinck, M. Lemmers, M. Van Montagu, and J. Schell.** 1982. Nucleotide sequence and transcript map of the *Agrobacterium tumefaciens* Ti plasmid-encoded octopine synthase gene. J. Mol. Appl. Genet. **1**:499–512.
10. **Denecke, J., V. Gosselé, J. Botterman, and M. Cornelissen.** 1989. Quantitative analysis of transiently expressed genes in plant cells. Methods Mol. Cell. Biol. **1**:19–27.
11. **French, R., and P. Ahlquist.** 1988. Characterization and engineering of sequences controlling in vivo synthesis of brome mosaic virus subgenomic RNA. J. Virol. **62**:2411–2420.
12. **Fromm, M., J. Callis, L. P. Taylor, and V. Walbot.** 1987. Electroporation of DNA and RNA into plant protoplasts. Methods Enzymol. **153**:351–366.
13. **Fütterer, J., and T. Hohn.** 1991. Translation of a polycistronic mRNA in the presence of the cauliflower mosaic virus transactivator protein. EMBO J. **10**:3887–3896.
14. **Gallie, D. R., W. J. Lucas, and V. Walbot.** 1989. Visualizing mRNA expression in plant protoplasts: factors influencing efficient mRNA uptake and translation. Plant Cell **1**:301–311.
15. **Gargouri, R., R. L. Joshi, J. F. Bol, S. Astier-Manifacier, and A. Haenni.** 1989. Mechanism of synthesis of turnip yellow mosaic virus coat protein subgenomic RNA *in vivo*. Virology **171**:386–393.
16. **Gorman, C. M., L. F. Moffat, and B. H. Howard.** 1982. Recombinant genomes which express chloramphenicol acetyltransferase in mammalian cells. Mol. Cell. Biol. **2**:1044–1051.
17. **Hacker, D. L., I. T. D. Petty, N. Wei, and T. J. Morris.** 1992. Turnip crinkle virus genes required for RNA replication and virus movement. Virology **186**:1–8.
18. **Hershey, J. W. B.** 1991. Translational control in mammalian cells. Annu. Rev. Biochem. **60**:717–755.
19. **Ishikawa, M., T. Meshi, T. Ohno, and Y. Okada.** 1991. Specific cessation of minus-strand RNA accumulation at an early stage of tobacco mosaic virus infection. J. Virol. **65**:861–868.
20. **Jefferson, R. A.** 1987. Assaying chimeric genes in plants: the GUS gene fusion system. Plant Mol. Biol. Rep. **5**:387–405.
21. **Jones, D. G., P. Dunsmuir, and J. Bedbrook.** 1985. High level expression of introduced chimaeric genes in regenerated transformed plants. EMBO J. **4**:2411–2418.
22. **Jones, I. M., and M. E. Reichmann.** 1973. The proteins synthesized in tobacco leaves infected with tobacco necrosis virus and satellite tobacco necrosis virus. Virology **52**:49–56.
23. **Joshi, C. P.** 1987. An inspection of the domain between putative TATA box and translation start site in 79 plant genes. Nucleic Acids Res. **15**:6643–6653.
24. **Kozak, M.** 1986. Point mutations define a sequence flanking the AUG initiator codon that modulates translation by eukaryotic ribosomes. Cell **44**:283–292.
25. **Kozak, M.** 1989. Context effects and inefficient initiation at non-AUG codons in eucaryotic cell-free translation systems. Mol. Cell. Biol. **9**:5073–5080.
26. **Krieg, P. A., and D. A. Melton.** 1984. Functional messenger RNAs are produced by SP6 *in vitro* transcription of cloned cDNAs. Nucleic Acids Res. **12**:7057–7070.
27. **Laemmli, U. K.** 1970. Cleavage of structural proteins during the assembly of the head of bacteriophage T4. Nature (London) **227**:680–685.
28. **Lehto, K., G. L. Grantham, and W. O. Dawson.** 1990. Insertion of sequences containing the coat protein subgenomic RNA promoter and leader in front of the tobacco mosaic virus 30K ORF delays its expression and causes defective cell-to-cell movement. Virology **174**:145–157.
29. **Lesnaw, J. A., and M. E. Reichmann.** 1969. The structure of tobacco necrosis virus. I. The protein subunit and the nature of the nucleic acid. Virology **39**:729–737.
30. **Marsh, L. E., C. C. Huntley, G. P. Pogue, J. P. Connell, and T. C. Hall.** 1991. Regulation of (+):(−)-strand asymmetry in replication of brome mosaic virus RNA. Virology **182**:76–83.
31. **Maxam, A. M., and W. Gilbert.** 1977. A new method for sequencing DNA. Proc. Natl. Acad. Sci. USA **74**:560–564.

32. **McKnight, S. L., E. R. Gavis, and R. Kingsbury.** 1981. Analysis of transcriptional regulatory signals of the HSV thymidine kinase gene: identification of an upstream control region. Cell **25:**385–398.
33. **McMaster, G. K., and G. G. Carmichael.** 1977. Analysis of single- and double-stranded nucleic acids on polyacrylamide and agarose gels by using glyoxal and acridine orange. Proc. Natl. Acad. Sci. USA **74:**4835–4838.
34. **Meulewaeter, F., J. Seurinck, and J. van Emmelo.** 1990. Genome structure of tobacco necrosis virus strain A. Virology **177:**699–709.
35. **Meulewaeter, F., and J. van Emmelo.** 1991. Expression of the coat protein gene of tobacco necrosis virus in transgenic tobacco plants. Med. Fac. Landbouwwet. Rijksuniv. Gent **56:** 595–600.
36. **Miller, W. A., T. W. Dreher, and T. C. Hall.** 1985. Synthesis of brome mosaic virus subgenomic RNA *in vitro* by internal initiation on (−)-sense genomic RNA. Nature (London) **313:**68–70.
37. **Morch, M. D., G. Drugeon, W. Zagorski, and A. L. Haenni.** 1986. The synthesis of high-molecular-weight proteins in the wheat germ translation system. Methods Enzymol. **118:**154–164.
38. **Munroe, D., and A. Jacobson.** 1990. Tales of poly(A): a review. Gene **91:**151–158.
39. **Nassuth, A., and J. F. Bol.** 1983. Altered balance of the synthesis of plus- and minus-strand RNAs induced by RNAs 1 and 2 of alfalfa mosaic virus in the absence of RNA 3. Virology **124:**75–85.
40. **Riviere, C. J., and D. M. Rochon.** 1990. Nucleotide sequence and genomic organization of melon necrotic spot virus. J. Gen. Virol. **71:**1887–1896.
41. **Sanger, F., S. Nicklen, and A. R. Coulson.** 1977. DNA sequencing with chain-terminating inhibitors. Proc. Natl. Acad. Sci. USA **74:**5463–5467.
42. **Van der Kuyl, A. C., K. Langereis, C. J. Houwing, E. M. J. Jaspars, and J. F. Bol.** 1990. *cis*-acting elements involved in replication of alfalfa mosaic virus RNAs *in vitro*. Virology **176:**346–354.
43. **Van der Kuyl, A. C., L. Neeleman, and J. F. Bol.** 1991. Deletion analysis of *cis*- and *trans*-acting elements involved in replication of alfalfa mosaic virus RNA 3 *in vivo*. Virology **183:**687–694.
44. **Van der Kuyl, A. C., L. Neeleman, and J. F. Bol.** 1991. Role of alfalfa mosaic virus coat protein in regulation of the balance between viral plus and minus strand RNA synthesis. Virology **185:**496–499.
45. **Velten, J., and J. Schell.** 1985. Selection-expression plasmid vectors for use in genetic transformation of higher plants. Nucleic Acids Res. **19:**6981–6998.
46. **Velten, J., L. Velten, R. Hain, and J. Schell.** 1984. Isolation of a dual promoter fragment from the Ti plasmid of *Agrobacterium tumefaciens*. EMBO J. **3:**2723–2730.
47. **Watanabe, Y., Y. Emori, I. Ooshika, T. Meshi, T. Ohno, and Y. Okada.** 1984. Synthesis of TMV-specific RNAs and proteins at the early stage of infection in tobacco protoplasts: transient expression of the 30K protein and its mRNA. Virology **133:**18–24.
48. **Watanabe, Y., and Y. Okada.** 1986. *In vitro* viral RNA synthesis by a subcellular fraction of TMV-infected tobacco protoplasts. Virology **149:**64–73.
49. **White, K. A., and G. A. Mackie.** 1990. Control and expression of 3′ open reading frames in clover yellow mosaic virus. Virology **179:**576–584.